Contribution from the Department of Chemistry,
University of Minnesota, Minneapolis, Minnesota 55455

Photochemistry of Dithiocarbamato Complexes. 3.[1] Photosensitized Reactions of Tris(*N*,*N*-dialkyldithiocarbamato)ruthenium(III) and the X-ray and Molecular Structure of Chlorobis(*N*,*N*-dimethyldithiocarbamato)(*N*,*N*-dimethylthiocarboxamido)ruthenium(IV)

G. L. Miessler and L. H. Pignolet*

Received June 26, 1978

The photochemistry of tris(*N*,*N*-dialkyldithiocarbamato)ruthenium(III), $Ru(R_2dtc)_3$ [R = Me or Et] in chlorocarbon solvents has recently been investigated.[2] The novel chlorine abstraction reaction which results from irradiation (λ 265–366 nm) of $Ru(R_2dtc)_3$ in $CHCl_3$ at 30 °C is summarized in eq 1. The compounds **1** and **2** which are formed simultaneously

$$Ru(R_2dtc)_3 \xrightarrow[CHCl_3]{h\nu} \underset{\mathbf{1}}{RuCl(R_2dtc)_3} + \underset{\mathbf{2}}{\alpha\text{-}[Ru_2(R_2dtc)_5]Cl} \qquad (1)$$

with **1** as the major product are the *only* ruthenium-containing products[2] and their structures have been determined by single-crystal X-ray analysis.[3,4] The photoreactivity of $Ru(R_2dtc)_3$ is believed to result from charge-transfer (CT) excitation[2] followed by electron transfer to chlorocarbon solvent and from charge-transfer-to-solvent excitation.[5] As part of our mechanistic study of this reaction, experiments were carried out using benzophenone as a triplet sensitizer for $Ru(R_2dtc)_3$ in $CHCl_3$ solvent. Unexpectedly, photolysis at 366 nm in the presence of a large molar excess of benzophenone produced an entirely new product in >90% yield. The new complex (R = Me) was characterized by single-crystal X-ray analysis and found to be $RuCl(Me_2dtc)_2(\eta^2\text{-}SCNMe_2)$, **3**.

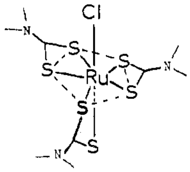

1

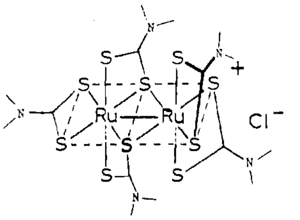

2

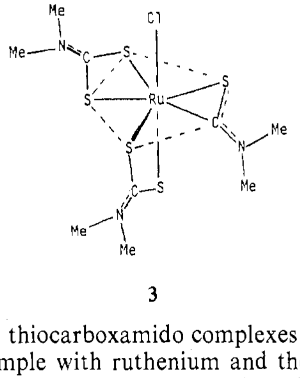

3

Although other thiocarboxamido complexes are known,[6,7] **3** is the first example with ruthenium and the only one synthesized photochemically from an R_2dtc ligand. The structure, synthesis, and properties of **3** are discussed in this paper.

Experimental Section

Preparation and Characterization of $RuCl(S_2CNMe_2)_2(SCNMe_2)$. $Ru(Me_2dtc)_3$, 0.0319 g, and 24.0 g of benzophenone were dissolved in 75 mL of $CHCl_3$ in a quartz flask in the dark. The solution was thoroughly degassed and placed under an atmosphere of purified Ar. The solution was then photolyzed for 24 h using a 450-W Hanovia Hg-vapor lamp and Corning filters 5860 and 7380 to isolate the 366-nm line. The concentrations of $Ru(Me_2dtc)_3$ and benzophenone were such that >90% of the 366-nm light was absorbed by benzophenone. After photolysis the dark brown color of the solution had changed to light reddish brown. After the $CHCl_3$ solvent was pumped off, the remaining residue was extracted repeatedly with pentane to remove the benzophenone. The orange solid which remained was found by NMR to contain ca. 10% $\alpha\text{-}Ru_2(Me_2dtc)_5^+$. This compound was removed by repeated recrystallizations from acetonitrile/toluene, followed by two recrystallizations from acetone/heptane to give orange needle-shaped crystals of $RuCl(S_2CNMe_2)_2(SCNMe_2)$ which showed traces of acetone, but no other impurities, by ^1H NMR. The decomposition point was 230 °C, and diamagnetism was indicated in the solid state (Faraday method) and in solution (NMR). IR (KBr): 2931, 1710 (acetone C=O), 1641, 1590 (thiocarboxamide $C \mathrel{\overset{\cdot\cdot}{-}} N$), 1532 ($Me_2dtc$ $C \mathrel{\overset{\cdot\cdot}{-}} N$), 1399, 1253, 1218, 1153, 983, 933, 821 cm^{-1}. ^1H NMR (CD_3CN, ambient temperature): δ 3.73 (relative intensity = 1), 3.52 (1), 3.20 (2), 3.17 (2). Electronic absorption spectrum ($CHCl_3$, 30 °C): λ_{max} 258 nm (ϵ 29 900 cm^{-1} M^{-1}), 475 nm (sh) (310). Conductivity in nitromethane at 25 °C: $\Lambda = 9.0\ \Omega^{-1}\ cm^2\ mol^{-1}$, indicating the compound to be weakly conducting (typical value for $RuCl(R_2dtc)_3$ is 22 $\Omega^{-1}\ cm^2\ mol^{-1}$).[3]

$RuCl(S_2CNEt_2)_2(SCNEt_2)$ was prepared in an identical manner to the R = Me compound. The decomposition point was 155 °C. IR (KBr): 2975, 2936, 1653, 1566 (thiocarboxamide $C \mathrel{\overset{\cdot\cdot}{-}} N$), 1504 ($Et_2dtc$ $C \mathrel{\overset{\cdot\cdot}{-}} N$), 1436, 1380, 1357, 1277, 1211, 1150, 1076, 1002, 944, 915, 900, 854, 808, 734, 701 cm^{-1}. The ^1H NMR spectrum (CD_3CN, ambient temperature) was a complex overlapping spectrum with multiplets centered as follows: δ 3.28 (quartet), 3.24 (quartet), 3.01 (quartet), 0.72 (triplet), 0.67 (triplet), 0.56 (triplet). Electronic absorption spectrum ($CHCl_3$, 30 °C): λ_{max} 258 nm, 335 (sh), 470 (sh).

Instrumentation. ^1H NMR spectra were recorded at 79.54 MHz using a Varian CFT 20 spectrometer. IR spectra were recorded in KBr disks with a Perkin-Elmer Model 237 grating spectrophotometer. Electronic absorption spectra were obtained in $CHCl_3$ solution at 25 °C with a Cary Model 14 spectrophotometer. Magnetic susceptibilities were determined by the Faraday method at 25 °C using $Hg[Co(SCN)_4]$ as calibrant. Conductivity experiments were carried out using a Yellow Springs Instrument Co. Model 31 conductivity bridge.

Quantum Yield Measurements. Quantum yields were measured in 1-cm quartz cells using a 100-W Hanovia Hg-vapor lamp with the sample housed in a thermostated box equipped with a magnetic stirrer. The 366-nm Hg line was isolated using an Optics Technology interference filter, No. 370, having maximum transmittance at 368 nm and a half-bandwidth of 34 nm. Intensities of the filtered light were measured by ferrioxalate actinometry as in our previous work.[1b]

The photosensitized quantum yield for the photolysis of $Ru(Et_2dtc)_3$ was determined as follows. A solution was prepared in the dark containing 0.58 M benzophenone and 1.5×10^{-4} M $Ru(Et_2dtc)_3$. The $CHCl_3$ had been passed down a basic alumina column immediately before use to remove traces of HCl. The solution was thoroughly degassed and placed under an atmosphere of purified Ar. A 3.0-mL sample was transferred to a 1-cm quartz cell and photolyzed (vide supra). Absorbance measurements were obtained at 560 and 470 nm at several time intervals during the first 10% of the reaction. These absorbance measurements, along with the extinction coefficients for $Ru(Et_2dtc)_3$, $RuCl(Et_2dtc)_3$, and $\alpha\text{-}[Ru_2(Et_2dtc)_5]Cl$, were used to calculate the concentration of $Ru(Et_2dtc)_3$ for each set of absorbance readings. The quantum yield reported is for the disappearance of $Ru(Et_2dtc)_3$ at 30 °C.

The photosensitized quantum yield for disappearance of $RuCl(Et_2dtc)_3$ was determined in a similar manner. A solution was prepared in the dark containing 0.60 M benzophenone and 1.4×10^{-4} M $RuCl(Et_2dtc)_3$ in $CHCl_3$. This solution was also degassed, and a 3.0-mL sample was transferred to a 1-cm cell for photolysis at 30 °C. Absorbance measurements were taken at 560 and 500 nm during the first 20% of the reaction. These measurements, along with the extinction coefficients of $RuCl(Et_2dtc)_3$ and $RuCl(S_2CNEt_2)_2(SCNEt_2)$, were used to calculate the rate of disappearance of $RuCl(Et_2dtc)_3$.

Structure Determination of $RuCl(S_2CNMe_2)_2(SCNMe_2)$. The crystal selected for the structural analysis was a parallelepiped of approximate dimensions 0.30 × 0.12 × 0.04 mm. It was mounted on the tip of a thin glass fiber and was fixed with 5-min epoxy.

0020-1669/79/1318-0210$01.00/0

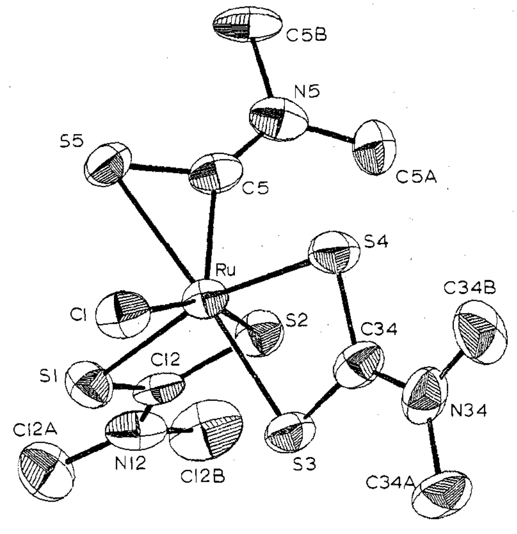

Figure 1. ORTEP drawing of the molecule $RuCl(S_2CNMe_2)_2(\eta^2\text{-}SCNMe_2)$. Ellipsoids are drawn at the 50% probability level.

Preliminary precession and cone-axis photographs revealed no symmetry and therefore the crystal was assumed to be triclinic.

The crystal was transferred to a Syntex $P2_1$ four-circle diffractometer controlled by a Nova 1200 computer and was accurately centered. The diffractometer used was located at Syntex Analytical Instruments, Cupertino, Calif., and was equipped with a molybdenum X-ray tube [λ(Mo K$\bar{\alpha}$) 0.71073] and a graphite monochromator. Twelve strong reflections, well dispersed in reciprocal space, were found by a random-orientation rotation photograph and were centered by the Syntex automatic centering routine. This procedure is described in ref 7. A triclinic cell was chosen by inspection from the automatic cell generation routine and axial photographs were taken about each of the three axes in order to confirm the choice of cell. The cell constants so determined were in agreement with the preliminary precession photographs and are a = 8.977 (2) Å, b = 9.369 (3) Å, c = 13.573 (6) Å, α = 93.54 (3)°, β = 99.05 (3)°, γ = 98.67 (2)°, and V = 1110 Å^3. The measured density, 1.55 g/cm^3, agrees with the calculated density, 1.566 g/cm^3, for Z = 2 and formula $RuClS_5C_9H_{18}N_3{\cdot}C_3H_6O$ (M_r = 523.2) for one asymmetric unit.

Intensity data were collected on the Syntex $P2_1$ four-circle diffractometer using the ω-scan technique.[8] Of the 3309 reflections collected out of 2θ = 45°, 2527 with intensity greater than $2\sigma(I)$[9] were used in solution and refinement of the structure. Three standard reflection intensities were checked at intervals of 50 sequential reflections and no significant changes were found.

Data were reduced to net intensities[9] and were not corrected for absorption (μ = 12.7 cm^{-1}). The intensity data were corrected for Lorentz and polarization effects. All calculations were performed by Syntex Analytical Instruments using the Syntex XTL structure determination system.[10] The positions of the ruthenium and several sulfur atoms were determined from a three-dimensional Patterson synthesis. The centrosymmetric space group $P\bar{1}$ was chosen and proved to be correct since the structure refined successfully. All nonhydrogen atoms were subsequently found after several Fourier and least-squares calculations. The acetone solvate molecule was located in a difference Fourier map and was found to be disordered (vide infra). NMR and IR spectra confirmed the presence of the acetone solvate. Final full-matrix least-squares refinement with all nonhydrogen atoms thermally anisotropic converged R_1 and R_2 to 0.055 and 0.066, respectively.[11]

The final atomic coordinates with their standard deviations and final thermal parameters with their standard deviations are given in Tables I and II. Figure 1 presents an ORTEP perspective of the molecular structure and shows the labeling scheme. A table of observed and calculated structure factors is available as supplementary material.

Table I. Final Atomic Fractional Coordinates with Standard Deviations

atom	x	y	z	B, Å^2
Ru	0.34501 (9)	0.35867 (8)	0.21538 (6)	a
S1	0.2733 (3)	0.5333 (3)	0.3273 (2)	a
S2	0.4476 (3)	0.5937 (3)	0.1753 (2)	a
S3	0.1386 (3)	0.3781 (3)	0.0846 (2)	a
S4	0.3499 (3)	0.1856 (3)	0.0772 (2)	a
S5	0.5361 (3)	0.3157 (3)	0.3567 (2)	a
Cl	0.1731 (3)	0.1679 (3)	0.2723 (2)	a
C12	0.3685 (10)	0.6647 (10)	0.2693 (7)	a
N12	0.3799 (9)	0.8081 (8)	0.2957 (6)	a
C12A	0.3162 (15)	0.8582 (12)	0.3808 (9)	a
C12B	0.4646 (14)	0.9123 (10)	0.2359 (9)	a
C34	0.1849 (11)	0.2348 (10)	0.0191 (7)	a
N34	0.1045 (10)	0.1693 (10)	−0.0675 (6)	a
C34A	−0.0411 (12)	0.2133 (13)	−0.1140 (8)	a
C34B	0.1526 (14)	0.0454 (12)	−0.1188 (8)	a
C5	0.5680 (10)	0.3491 (10)	0.2459 (7)	a
N5	0.6893 (9)	0.3599 (9)	0.2010 (7)	a
C5A	0.6888 (13)	0.4023 (14)	0.0968 (8)	a
C5B	0.8391 (10)	0.3413 (14)	0.2626 (9)	a
X1[b]	0.8849 (21)	0.7568 (19)	0.3296 (14)	10.2 (5)
X2[b]	0.8511 (30)	0.7585 (28)	0.4076 (20)	14.0 (7)
X3[b]	0.7149 (26)	0.7417 (22)	0.4504 (15)	13.7 (6)
X4[b]	0.9383 (32)	0.6511 (28)	0.4743 (19)	18.7 (9)
X5[b]	0.8664 (38)	0.9288 (37)	0.4255 (22)	27.1 (12)

[a] Refined anisotropically; see Table II. [b] Disordered acetone molecule; see text.

Table II. Anisotropic Thermal Parameters[a] with Standard Deviations

atom	β_{11}	β_{22}	β_{33}	β_{12}	β_{13}	β_{23}
Ru	2.91 (4)	3.63 (4)	3.56 (4)	0.68 (3)	0.18 (3)	0.42 (3)
S1	4.2 (1)	3.7 (1)	4.3 (1)	1.0 (1)	1.2 (1)	0.16 (9)
S2	3.8 (1)	3.6 (1)	4.1 (1)	0.4 (1)	0.6 (1)	0.93 (9)
S3	3.2 (1)	4.4 (1)	4.0 (1)	1.0 (1)	−0.2 (1)	0.4 (1)
S4	3.7 (1)	4.3 (1)	4.2 (1)	1.3 (1)	−0.2 (1)	−0.5 (1)
S5	3.6 (1)	5.4 (1)	3.4 (1)	0.9 (1)	−0.1 (1)	1.0 (1)
Cl	3.3 (1)	3.8 (1)	5.3 (1)	0.0 (1)	0.4 (1)	0.9 (1)
C12	2.7 (4)	4.4 (4)	4.2 (4)	1.4 (3)	−0.5 (3)	1.0 (3)
N12	4.0 (4)	3.9 (4)	6.3 (5)	1.6 (3)	0.0 (3)	0.6 (3)
C12A	8.9 (7)	5.2 (5)	5.8 (6)	3.2 (5)	1.7 (5)	−0.9 (4)
C12B	6.8 (6)	3.4 (4)	9.0 (7)	−0.2 (4)	0.5 (6)	2.6 (4)
C34	3.4 (4)	4.3 (4)	3.9 (4)	0.0 (3)	−0.3 (4)	1.0 (3)
N34	4.5 (4)	6.5 (4)	3.2 (3)	−0.1 (4)	−0.2 (3)	0.0 (3)
C34A	4.2 (5)	8.0 (7)	5.0 (5)	1.7 (5)	−1.7 (4)	−0.3 (5)
C34B	6.9 (7)	6.5 (6)	5.0 (5)	1.0 (5)	1.0 (5)	−2.3 (5)
C5	2.9 (4)	3.3 (4)	4.5 (5)	0.3 (3)	−0.3 (4)	0.3 (3)
N5	3.2 (4)	6.0 (4)	6.1 (5)	1.2 (3)	0.6 (3)	0.5 (4)
C5A	5.5 (6)	9.6 (7)	4.1 (5)	2.3 (5)	2.1 (4)	2.1 (5)
C5B	2.6 (3)	11.7 (8)	7.8 (7)	3.5 (5)	−0.3 (4)	1.5 (6)

[a] These anisotropic thermal parameters are analogous to the usual form of the thermal parameter and have units of Å^2. They enter the expression for the structure factor in the form exp$[-0.25(\beta_{11}h^2a^{*2} + \beta_{22}k^2b^{*2} + \beta_{33}l^2c^{*2} + \beta_{12}hka^*b^* + 2\beta_{13}{\cdot}kla^*c^* + 2\beta_{23}klb^*c^*)]$.

Results and Discussion

The spectroscopic and magnetic characterization data presented in the Experimental Section suggested that **3** was either a new complex of Ru(IV), similar to **1**, or a bimetallic complex of Ru(III), similar to **2**. The results of a single-crystal X-ray study clearly showed the compound to be a monomeric complex of Ru(IV) with the formulation $RuCl(S_2CNMe_2)_2(\eta^2\text{-}SCNMe_2)$. The structure, which is shown in Figure 1, is best described as a distorted pentagonal bipyramid (PBP) with the equatorial pentagon containing S1, S3, S4, S5, and C5 and with axial positions Cl and S2. The structure is similar to that of **1**;[3] however, it is significantly more distorted in the equatorial plane due primarily to the small bite angle of the chelating η^2-thiocarboxamido ligand [S5–Ru–C5 40.8 (3)°]. The PBP geometry is now well established for diamagnetic M(chelate)$_3$X complexes of Ru(IV).[12,13] The important distances and angles in **3** are presented in Tables III and IV.

The two Me$_2$dtc ligands have normal distances and angles compared with those of numerous other Me$_2$dtc structures.[3]

Table III. Interatomic Distances and Angles in the RuS_5CCl Core[a]

	Distances, Å		
Ru-S1	2.391 (3)	S1-S2	2.812 (4)
Ru-S2	2.384 (3)	S3-S4	2.816 (4)
Ru-S3	2.392 (3)	Cl-S5	3.333 (4)
Ru-S4	2.414 (3)	Cl-C5	3.771 (10)
Ru-S5	2.459 (3)	Cl-S1	3.411 (3)
Ru-Cl	2.425 (3)	Cl-S3	3.318 (4)
Ru-C5	1.996 (10)	Cl-S4	3.295 (4)
S5-C5	1.614 (10)	S2-S3	3.197 (4)
S2-C5	2.833 (9)	S2-S4	3.894 (4)
S4-C5	2.946 (10)	S2-S5	3.776 (4)
S1-S3	3.472 (4)	S1-S5	3.336 (4)
	Angles, deg		
S1-Ru-S2	72.15 (9)	Cl-Ru-S1	90.17 (9)
S3-Ru-S4	71.74 (9)	Cl-Ru-S3	87.06 (9)
S5-Ru-C5	40.8 (3)	Cl-Ru-S4	85.81 (9)
S4-Ru-C5	83.3 (3)	Cl-Ru-C5	116.8 (3)
S1-Ru-S5	86.90 (9)	Cl-Ru-S5	86.07 (9)
S1-Ru-S3	93.08 (9)	S2-Ru-S3	84.03 (9)
Ru-S5-C5	54.0 (3)	S2-Ru-S4	108.50 (9)
Ru-C5-S5	85.2 (4)	S2-Ru-S5	102.47 (9)
Cl-Ru-S2	159.67 (9)	S2-Ru-C5	80.1 (3)
S1-Ru-S4	164.5 (1)	S3-Ru-S5	173.13 (9)
		S4-Ru-S5	107.76 (9)

[a] For numbering system, see Figure 1.

Table IV. Interatomic Distances and Angles in the Ligands[a]

	ligand 1-2	ligand 3-4	ligand 5
		Distances, Å	
S(1,3,5)-C	1.695 (10)	1.704 (10)	1.614 (10)
S(2,4)-C	1.702 (9)	1.706 (10)	
C-N	1.35 (1)	1.34 (1)	1.32 (1)
N-C(A)	1.45 (2)	1.49 (1)	1.49 (1)
N-C(B)	1.50 (1)	1.47 (1)	1.51 (1)
		Angles, deg	
Ru-S(1,3)-C	88.0 (3)	88.6 (3)	
Ru-S(2,4)-C	88.1 (3)	87.8 (3)	
S(1,3)-C-S(2,4)	111.7 (5)	111.4 (5)	
S(1,3,5)-C-N	123.6 (7)	125.0 (8)	135.0 (8)
S(2,4), Ru-C-N	124.7 (7)	123.6 (7)	139.8 (7)
C-N-C(A)	120.7 (9)	121.8 (8)	123.8 (9)
C-N-C(B)	117.7 (8)	121.4 (9)	117.4 (9)
C(A)-N-C(B)	121.5 (9)	116.8 (8)	118.5 (9)

[a] For numbering system, see Figure 1.

The average Ru–S(dtc) distance (2.395 Å) is identical with that found in **1**, and the Ru–Cl distance is long compared with those of other ruthenium complexes but is quite similar to the distance found in **1**.[3] The Cl–S nonbonded distances range from 3.20 to 3.41 Å with an average value of 3.34 Å. All of these distances are short compared with the Cl–S van der Waals contact distance of 3.65 Å[14] and this probably accounts for the long Ru–Cl distance and the partial ionic nature of **3** in polar solvents. The thiocarboxamido ligand is now well-known and its chelating η^2-coordinating geometry has been thoroughly discussed.[6,15] The distances and angles in the η^2-$SCNMe_2$ group in **3** are normal and not significantly different from those found in $RhCl(Me_2dtc)(\eta^2\text{-}SCNMe_2)(PPh_3)$,[16] $RhCl[PhNC(S)NMe_2](\eta^2\text{-}SCNMe_2)(PPh_3)$,[17] and $[Ir(\eta^2\text{-}SCNMe_2)_2(CO)(PPh_3)]^+$.[6a] The Ru–S distance to the η^2-$SCNMe_2$ ligand [2.459 (3) Å] is somewhat longer than the Me_2dtc Ru–S distances (average 2.395 Å), while the η^2-$SCNMe_2$ C–S distance [1.61 (1) Å] is shorter than the Me_2dtc C–S distances (average 1.70 Å). This is characteristic of mixed R_2dtc–η^2-$SCNR_2$ complexes.[6c,16,18] The Ru–C distance in **3** [2.00 (1) Å] is slightly longer than expected, compared with values of 1.90 (2) and 1.96 (2) Å observed in the two six-coordinate Rh complexes listed above, respectively,[16,17] but is quite similar to the Ir–C distance (average 1.99 Å).[6a] Slightly longer metal–ligand distances are expected for seven-coordinate complexes compared with those of six-coordinate analogues, and this has also been observed with the Ru–S distances in $RuCl(Et_2dtc)_3$ compared with those of $Ru(Et_2dtc)_3$.[3]

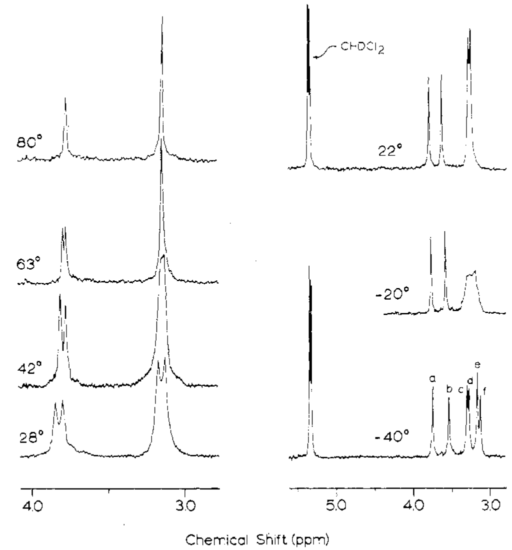

Figure 2. Variable-temperature ^1H NMR spectra of $RuCl(S_2CNMe_2)_2(\eta^2\text{-}SCNMe_2)$ recorded in CD_2Cl_2 (−40 to +22 °C) and $C_6D_5NO_2$ (+28 to +80 °C) solution at 79.54 MHz. Chemical shifts are relative to Me_4Si.

Complexes containing thiocarboxamido ligands have most often been synthesized by oxidative addition of dialkylthiocarbamoyl chloride, $R_2NC(S)Cl$, to low oxidation state metal–phosphine or –carbonyl complexes.[6a,6c,15,19] There are reports, however, of C–S bond cleavage in the dithiocarbamate ester $[MeSC(S)NMe_2]$ and in tetramethylthiuram monosulfide $[Me_2NC(S)SC(S)NMe_2]$ by $RhCl(PPh_3)_3$ leading to formation of $RhCl(SMe)(SCNMe_2)PPh_3$ and $RhCl(S_2CNMe_2)(SCNMe_2)PPh_3$, respectively.[6b] In only one case has a thiocarboxamido complex been prepared directly from an R_2dtc ligand. Reaction of the *N*,*N*-di-*n*-propyldithiocarbamate ion with molybdenum(II) acetate formed the bimetallic complex $[Mo(\eta^2\text{-}SCNPr_2)(S_2CNPr_2)S]_2$.[18] The photochemical synthesis of **3** is therefore quite novel.

Although further experimentation is necessary in order to determine the mechanism of the photosensitized production of **3** from $Ru(R_2dtc)_3$, several important aspects of the reaction can be stated. The quantum yield for the benzophenone-sensitized formation of **3** (R = Et) as determined by the disappearance of $Ru(Et_2dtc)_3$ is 0.30 at λ 366 nm (30 °C in $CHCl_3$) while the quantum yield for the unsensitized reaction (eq 1) is only 0.01 at 366 nm.[2] Additionally, the quantum yield for conversion of **1** into **3** in the presence of benzophenone is 0.50 at 366 nm (30 °C in $CHCl_3$), and **1** is observed by ^1H NMR spectroscopy during the early stages of the photosensitized conversion of $Ru(Et_2dtc)_3$ into **3**. Therefore it is very likely that the conversion of $Ru(Et_2dtc)_3$ into **1** is also photosensitized and is the first step in the formation of **3**. The photochemical formation of $FeCl(R_2dtc)_2$ from $Fe(R_2dtc)_3$ and $CHCl_3$ is also significantly photosensitized by benzophenone at λ 366 nm (sensitized and unsensitized ϕ = 0.47 and 0.050, respectively).[1b] Experiments in progress are aimed at determining the mechanism of the photosensitized loss of sulfur from **1** and the chlorine abstraction by $Ru(R_2dtc)_3$.

The $RuCl(S_2CNMe_2)_2(\eta^2\text{-}SCNMe_2)$ molecule is nonrigid in solution, as shown by its variable-temperature ^1H NMR spectra (Figure 2). At −40 °C, the six nonequivalent methyl resonances a–f, which are expected assuming the solid-state geometry (Figure 1 and 3), are resolved. Two distinct dynamic processes are apparent which cause coalescence of peaks c–f at ca. −20 and +42 °C. Peaks a and b do not necessarily coalesce but possibly become accidently degenerate at ca. 80 °C; however, at higher temperatures (100 °C) the resonances do not again show nonequivalence, as might be expected for accidental degeneracy. Since the barrier to C=N bond rotation in the thiocarboxamido ligand is expected to be much higher than for $S_2C{=}N$ bond rotation[19,20] and because of the overall coalescence pattern and intensities, peaks a and b are assigned to the η^2-$SCNMe_2$ ligand. Additionally, the −20 °C coalescence is most likely due to $S_2C{=}N$ bond rotation[20] while the 42 °C coalescence probably results from fast Me_2dtc scrambling via a metal-centered rearrangement process. The complexes $RuX(R_2dtc)_3$, where X = Cl (**1**) or I, are nonrigid at −90 °C such that all R_2dtc ligands appear equivalent. Possible mechanisms for this process have been discussed.[3] It is certainly possible that a similar ligand scrambling occurs in **3**; however, it is not clear why the presence of the η^2-$SCNMe_2$ ligand significantly increases the barrier to this rearrangement. The coalescence of peaks a and b at ca. 80 °C must result from C=N bond rotation in the η^2-$SCNMe_2$ ligand; however, the possibility of accidental degeneracy cannot be eliminated (vide supra).

Acknowledgment. This research was supported by the National Science Foundation. We are grateful to Dr. Arild Christensen and to Syntex Analytical Instruments for carrying out the X-ray analysis. We thank Engelhard Industries for a loan of $RuCl_3$.

Registry No. **3**, 68200-83-9; $Ru(Me_2dtc)_3$, 43190-67-6; $RuCl(S_2CNEt_2)_2(SCNEt_2)$, 68200-84-0.

Supplementary Material Available: A table of observed and calculated structural factor amplitudes (19 pages). Ordering information is given on any current masthead page.

References and Notes

(1) (a) Part 1: G. L. Miessler, G. Stuk, T. P. Smith, K. W. Given, M. C. Palazzotto, and L. H. Pignolet, *Inorg. Chem.*, **15**, 1982 (1976). (b) Part 2: G. L. Miessler, E. Zoebisch, and L. H. Pignolet, *ibid.*, **17**, 3636 (1978).

(2) K. W. Given, B. M. Mattson, M. F. McGuiggan, G. L. Miessler, and L. H. Pignolet, *J. Am. Chem. Soc.*, **99**, 4855 (1977).

(3) K. W. Given, B. M. Mattson, and L. H. Pignolet, *Inorg. Chem.*, **15**, 3152 (1976).

(4) A. R. Hendrickson, J. M. Hope, and R. L. Martin, *J. Chem. Soc., Dalton Trans.*, 2032 (1976).

(5) G. L. Miessler, M. F. McGuiggan, and L. H. Pignolet, paper in preparation.

(6) See for example: (a) A. W. Gal, Ph.D. Thesis, University of Nijmegen, Toernooiveld, Nijmegen, The Netherlands, 1977; (b) A. W. Gal, A. F. J. M. van der Ploeg, F. A. Vollenbroek, and W. Bosman, *J. Organomet. Chem.*, **96**, 123 (1975); (c) W. K. Dean and D. G. van der Veer, *ibid.*, **144**, 65 (1978); (d) G. R. Clark, T. J. Collins, D. Hall, S. M. James, and W. R. Roper, *ibid.*, **141**, C5 (1977), and references cited therein.

(7) M. R. Churchill, R. A. Lashewycz, and F. J. Rotella, *Inorg. Chem.*, **16**, 265 (1977).

(8) Data collection was carried out by Dr. Arild Christensen of Syntex Analytical Instruments, Cupertino, Calif.

(9) Data were reduced to net intensities (I) and their esd's ($\sigma(I)$) according to the equations $I = CT - \tau(B_1 + B_2)$ and $\sigma(I) = [CT + \tau^2(B_1 + B_2)]^{1/2}$, where CT is the count during the scan, τ is the ratio of scan time to background time (=1 in the present case) and B_1 and B_2 are the initial and final backgrounds.

(10) "Syntex XTL Operations Manual", 2nd ed., Syntex Analytical Instruments, Cupertino, Calif., 1976.

(11) $R_1 = \sum||F_o| - |F_c||/\sum|F_o|$, $R_2 = [\sum w(|F_o| - |F_c|)^2/\sum w|F_o|^2]^{1/2}$; the numerator of R_2 was the function minimized; the weights were $w = [\sigma(|F_o|)]^{-2}$, where $\sigma(F_o)^2 = \sigma(I)/Lp$. Atomic scattering factors were taken from "International Tables for X-ray Crystallography", Vol. IV, Kynoch Press, Birmingham, England, 1974. Anomalous dispersion corrections from the same source were used for Ru, Cl, and S.

(12) B. M. Mattson and L. H. Pignolet, *Inorg. Chem.*, **16**, 488 (1977).

(13) S. H. Wheeler, B. M. Mattson, G. L. Miessler, and L. H. Pignolet, *Inorg. Chem.*, **17**, 340 (1978).

(14) L. Pauling, "The Nature of the Chemical Bond", 3rd ed., Cornell University Press, Ithaca, N.Y., 1960, p 260.

(15) W. K. Dean, R. S. Charles, and D. G. van der Veer, *Inorg. Chem.*, **16**, 3328 (1977).

(16) W. P. Bosman and A. W. Gal, *Cryst. Struct. Commun.*, **5**, 703 (1976).

(17) W. P. Bosman and A. W. Gal, *Cryst. Struct. Commun.*, **4**, 465 (1975).

(18) L. Ricard, J. Estienne, and R. Weiss, *Inorg. Chem.*, **12**, 2182 (1973).

(19) W. K. Dean, *J. Organomet. Chem.*, **135**, 195 (1977), and references cited therein.

(20) B. L. Edgar, D. J. Duffy, M. C. Palazzotto, and L. H. Pignolet, *J. Am. Chem. Soc.*, **95**, 1125 (1973); L. H. Pignolet, *Top. Curr. Chem.*, **56**, 91 (1975).

Contribution from the Anorganisch-Chemisches Institut der Universität, Göttingen, West Germany

$CF_3CF_2N{=}SF_2$—A Precursor of Five- and Six-Member Heterocycles

O. Glemser and Jean'ne M. Shreeve*[1]

Received August 31, 1978

While taking advantage of the facile route for the synthesis of five-member heterocycles which contain three-coordinate sulfur(IV) via the reaction of pentafluoroethyliminosulfur difluoride with amines[2,3] and diols, viz.

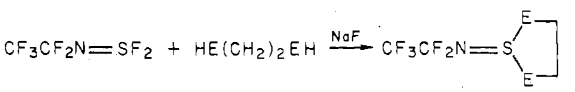

E = NCH_3; O

we observed that the reaction with 2-mercaptoethanol did not produce an analogous product. Instead a slightly volatile colorless liquid, in addition to solid $CF_3C(O)NH_2$, was formed at room temperature and was removed under dynamic vacuum (eq 1). Since traces of CF_3CN were known to be present in the $CF_3CF_2N{=}SF_2$, we examined the reaction of the 2-mercaptoethanol with this nitrile. None of the 2-trifluoromethyl-1,4,3-oxathiazine was formed. It was shown subsequently that carefully purified $CF_3CF_2N{=}SF_2$ behaves as in (1).

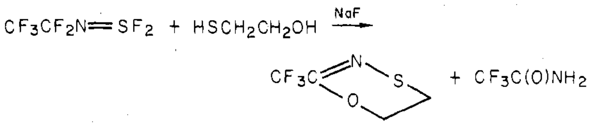

(1)

The formation of $CF_3\overline{C{=}NSCH_2CH_2O}$ is unexpected. It was separated from the $CF_3C(O)NH_2$ by repeated sublimations. When the solid residue from the reaction was extracted with anhydrous CH_2Cl_2, and the solid remaining, after evaporation of CH_2Cl_2, was heated at 60°C under high vacuum, a slightly volatile liquid and solid were distilled off. These products were not separated. The most distinguishing feature seen in the infrared spectrum of the mixture is a very intense band at 1787 cm^{-1} which likely arises from $\nu_{C=O}$. Additional bands fall in the O–H, C–H, and C–F stretching regions.

Spectral data are very useful in assigning the correct structure for these new heterocycles, particularly for the unexpected oxathiazine. In the infrared spectrum of $CF_3\overline{C{=}NSCH_2CH_2O}$, a strong band at 1657 cm^{-1} is assigned to $\nu_{C=N}$. There is no activity in the ν_{N-H} region. A molecule ion is observed in the mass spectrum, and a peak assigned to CF_3CO^+ supports a structure with C–O and N–S bonding. In the nuclear magnetic resonance spectra, a singlet CF_3 resonance and two proton resonances of equal area, which can be assigned to CH_2O and CH_2S, are found.

Experimental Section

All gases, volatile liquids, and sublimable solids were handled in a conventional glass vacuum apparatus. Pentafluoroethyliminosulfur